Climatic Change (2021) 166: 1
https://doi.org/10.1007/s10584-021-03094-0

Global trends in the frequency and duration of temperature extremes

Frank A. La Sorte[1] · Alison Johnston[1] · Toby R. Ault[2]

Received: 4 June 2020 / Accepted: 7 April 2021 / Published online: 1 May 2021

Abstract

Anthropogenic climate change has affected the frequency and duration of extreme climate events, including extreme heat events (EHE) and extreme cold events (ECE). How the frequency and duration of both EHE and ECE have changed over time within both terrestrial and marine environments globally has not been fully explored. Here, we use detrended daily estimates of minimum and maximum temperature from the ERA5 reanalysis over a 70-year period (1950–2019) to estimate the daily occurrence of EHE and ECE across the globe. We measure the frequency and duration of EHE and ECE by season across years and estimate how these measures have changed over time. Frequency and duration for both EHE and ECE presented similar patterns characterized by low spatial heterogeneity and strong seasonal variation. High EHE frequency and duration occurred within the Antarctic during the austral summer and winter and within the Arctic Ocean during the boreal winter. High ECE frequency and duration occurred within the Nearctic and Palearctic during the boreal winter and the Arctic Ocean during the boreal summer. The trend analysis presented pronounced differences between frequency and duration, high spatial heterogeneity, especially within terrestrial environments, and strong seasonal variation. Positive EHE trends, primarily in duration within marine environments, occurred during the boreal summer within the mid-latitudes of the Northern Hemisphere and during the austral summer within the mid-latitudes of the Southern Hemisphere. The eastern tropical Pacific contained positive EHE and ECE trends, primary in duration during the boreal winter. Our findings emphasize the many near-term challenges that extreme temperature events are likely to pose for human and natural systems within terrestrial and marine environments, and the need to advance our understanding of the developing long-term implications of these changing dynamics as climate change progresses.

Keywords Cold-air outbreaks · Climate change · Climate extremes · Detrended temperature · Heat waves · Temperature extremes

✉ Frank A. La Sorte
fal42@cornell.edu

[1] Cornell Lab of Ornithology, Cornell University, Ithaca, NY 14850, USA

[2] Department of Earth and Atmospheric Sciences, Cornell University, Ithaca, NY 14853, USA

1 Introduction

Anthropogenic climate change is affecting the frequency and duration of extreme climate events (AghaKouchak et al. 2020; Diffenbaugh et al. 2017). These extreme events encompass a variety of phenomena including extreme heat events (EHE) (Alexander et al. 2006; Coumou and Robinson 2013; Fischer and Knutti 2015) and extreme cold events (ECE) (Walsh et al. 2001; Wheeler et al. 2011). There is evidence that exposure to EHE adversely affects human populations (Anderson and Bell Michelle 2011; Battisti and Naylor 2009; Guo et al. 2017; Mitchell et al. 2016) and natural systems within terrestrial (Harris et al. 2018; Maxwell et al. 2019) and marine environments (Garrabou et al. 2009; Wernberg et al. 2013). There is similar evidence that ECE adversely affects human populations (Smith and Sheridan 2019) and natural systems within terrestrial environments (Maxwell et al. 2019). For species in natural systems, EHE and ECE can further the decline and extirpation of populations, increasing the chances of extinction (Maron et al. 2015; Maxwell et al. 2019). EHE and ECE can also promote the formation of novel ecosystems (Harris et al. 2018), generate enhanced selection pressures (Grant et al. 2017; Gutschick and BassiriRad 2003), and change the phenology of life history events (Cremonese et al. 2017; La Sorte et al. 2016).

How the frequency and duration of EHE has changed over time has been explored primarily within terrestrial regions during the boreal and austral summers (Coumou and Robinson 2013; Oswald 2018; Perkins-Kirkpatrick and Lewis 2020), but there are examples that have considered other seasons of the year (Alexander et al. 2006). Within marine environments, the primary focus has been on documenting "marine heatwaves" or extreme warming in sea surface temperatures. Marine heatwaves have increased in frequency and duration across the globe (Frölicher et al. 2018; Oliver et al. 2018). These events have significantly affected the composition and structure of marine ecosystems (Smale et al. 2019). Sea surface temperatures tend to be higher and less variable on average compared to air temperatures measured on the ocean's surface (Cayan 1980). Research examining the frequency and duration of ECE has focused primarily on cold-air outbreaks within the North Hemisphere during the boreal winter (Kolstad et al. 2010; Kretschmer et al. 2018). In total, how the frequency and duration of EHE and ECE have changed over time within both terrestrial and marine environments globally has not been fully explored.

There are a number of climate indices that have been used to estimate the occurrence of EHE (Fenner et al. 2019; Smith et al. 2013) and ECE (Smith and Sheridan 2018). These indices are often context specific, and there is little consensus on the most appropriate technique (McPhillips et al. 2018). Here, we define the occurrence of EHE and ECE using a probabilistic framework that estimates the novelty of each event relative to historical year-to-year variation in minimum and maximum temperature. We use detrended daily measures of minimum and maximum temperature to estimate when and where conditions significantly exceed historical variation over a 70-year period (1950 to 2019) during two seasons of the year. The more unusual the event relative to historical variation, the more likely it will adversely affect human and natural systems (Williams and Jackson 2007; Williams et al. 2007). This approach provides a standardized method for assessing the novelty of temperature extremes that minimizes the influence of global warming. We use this approach to determine how the frequency and duration of EHE and ECE have changed over time by season across the globe, and we identify the regions and seasons where these events are likely to have the most significant effects on natural and human populations now and into the future.

2 Materials and methods

We compiled gridded climate data from the European Centre for Medium-Range Weather Forecasts (ECMWF) fifth generation atmospheric reanalysis of the global climate (ERA5) (Hersbach et al. 2019b; Hoffmann et al. 2019). Key improvements provided by ERA5 over its predecessor includes broader data assimilation, improvements in global radiation budgets, better representation of tropospheric circulation, enhanced spatial and temporal resolutions, improved temporal consistency, and the ability to better resolve extreme events (Hersbach et al. 2019b). Reanalysis products rely on data assimilation where observations and model-based forecasts are used to generate spatially comprehensive estimates of climate variables at regular intervals over long time periods (Parker 2016). These characteristics are beneficial when estimating global trends in the frequency and duration of temperature extremes. The chief difference between reanalysis products and related climate observations is that the errors and uncertainties associations with reanalysis products are often less well understood (Parker 2016).

For our analysis, we used the ERA5 climate variable hourly air temperature at 2 m above the surface gridded at a 31 km (0.28125° at the equator) spatial resolution over a 70-year period: 1950 to 1978 (Bell et al. 2020) and 1979 to 2019 (Hersbach et al. 2019a). We used hourly air temperature to first extract the minimum and maximum temperature for each day and grid cell over the 70-year period. To reduce the influence of warming trends on our analysis, we detrended the 70-year time series of minimum and maximum temperature separately for each day and grid cell using the Complete Ensemble Empirical Mode Decomposition with Adaptive Noise (CEEMDAN) procedure (Torres et al. 2011). CEEMDAN is a variant of the Ensemble Empirical Mode Decomposition (EEMD) procedure (Wu and Huang 2009), which is a white noise-assisted refinement of the Empirical Mode Decomposition (EMD) procedure (Huang et al. 1998; Wu et al. 2007). EMD is a highly adaptive method that is well suited to decompose non-stationary and non-linear time series. EMD has been broadly applied in climate research and is an effective method for identifying the primary characteristics of global warming (Molla et al. 2007). The EMD procedure partitions time series into intrinsic modes of oscillation (Intrinsic Mode Functions; IMFs) based on the principle of local scale separation (Huang et al. 1998; Wu et al. 2007). The IMFs are extracted level by level until no complete oscillation can be identified. EEMD consists of "sifting" an ensemble of white noise-added signal, and CEEMDAN provides an exact reconstruction of the original signal and a better spectral separation of the IMFs. The residuals that remain after the implementation of the IMF partitioning procedure define a monotonic time series that can be used to detrend the original data. In this case, we detrended the 70-year time series by subtracting the minimum temperature CEEMDAN residuals (Fig. S1) from observed minimum temperature and the maximum temperature CEEMDAN residuals (Fig. S2) from observed maximum temperature by day within each grid cell. Factors that can limit the value of EMD as a detrended procedure include end effects and the presence of high stochasticity in the time series (Stallone et al. 2020). The CEEMDAN variant reduces the influence of end effects (Wu and Huang 2009) and is more efficient in recovering signals from noisy data (Colominas et al. 2012).

We used the following method to estimate the occurrence of extreme heat events (EHE) and extreme cold events (ECE) for each day and grid cell over the 70-year time series (Fig. S3). We treated the detrended minimum and maximum temperature values as normally distributed across years for each day and grid cell, an assumption that our data achieved in most cases (Fig. S4). We estimated the probability density function for minimum and maximum temperature using the mean and standard deviation calculated across years for each day and grid cell.

EHE occurred when the probabilities for both minimum and maximum temperature on a given day within a given grid cell were within the 0.025 quantile of the right tail (0.975–1.00) of the two probability density functions (Fig. S3). ECE occurred when the probabilities for both minimum and maximum temperature on a given day within a given grid cell were within the 0.025 quantile of the left tail (0.00–0.025) of the two probability density functions (Fig. S3). This approach follows from previous studies where interannual climatic variation is used to identify climatic novelty (La Sorte et al. 2018; Williams et al. 2007). Here, we used interannual variation in the 70-year time series of detrended minimum and maximum temperature data to determine when both minimum and maximum temperature achieved unusually high or low levels. This approach tends to capture multiday EHE and ECE events that occur over large geographic regions (see Appendix 1).

We summarized EHE and ECE for each year and grid cell using two measures. We applied these measures to two seasons: an extended boreal summer or austral winter (May–September) and an extended boreal winter or austral summer (November–March). The first measure estimated the frequency of extreme events based on the proportion of days within each season containing each event per year within each grid cell. The second estimated the duration of sequential events within each season per year within each grid cell. For the first measure, we calculated the proportion of days by season for each year and grid cell where an event occurred. To provide a spatial summary, we averaged the proportion of days by season containing each event across years for each grid cell. This approach identified grid cells that had high numbers of extreme events across years. To summarize the time series for this measure, we modeled the trend in the proportion of days for each event by season across years using beta regression with a logit link function and an identity function in the precision model (Ferrari and Cribari-Neto 2004; Simas et al. 2010). We removed zeros and ones using the transformation $(y\,(n-1)+0.5)\,/\,n$ where y is the vector of proportions and n is the sample size (Smithson and Verkuilen 2006). We selected beta regression because it is well suited to model continuous proportions whose values occur in the standard unit interval (0, 1). The probability density function of the beta distribution can take on a wide variety of different shapes, providing the flexibility necessary to model continuous proportions across many settings. Unlike traditional linear regression, beta regression enhances interpretability and inferential quality (Ferrari and Cribari-Neto 2004).

Our second measure estimated the duration of each extreme event by season for each year and grid cell based on the number of consecutive days containing EHE or ECE. For our analysis, we extracted the maximum duration of EHE and ECE for each season, year, and grid cell. This approach identified the longest extreme event that occurred during each year. We selected the maximum because duration tended to be strongly right skewed. To provide a spatial summary, we averaged the maximum duration of each event across years by season and grid cell. To summarize the time series of this measure, we modeled the trend in maximum duration for each event across years by season using Poisson regression (Lambert 1992). We selected Poisson regression because our measure of duration (number of days) is a non-negative integer that can be interpreted as a count. Applying traditional linear regression to count data often violates the model's assumptions, resulting in less robust inferences (Warton et al. 2016).

To provide a regional summary of our two measures, we calculated the median values from our spatial summaries and trend analyses for each measure by season within seven biogeographical realms (Olson and Dinerstein 2002; Pielou 1979) and seven oceans (Flanders Marine Institute 2018). Only grid cells within each realm and ocean where $P < 0.05$ were included in the trendcalculations. We included ±2 median absolute deviations with each median value,

which approximates the 95% confidence interval, to provide a context to assess the level of evidence for statistically significant differences.The seven biogeographical realms included the Afrotropics, Antarctic, Australasia, IndoMalaya, Nearctic, Neotropics, and Palearctic. The seven oceans included the Arctic, Indian, North Atlantic, North Pacific, South Atlantic, South Pacific, and Southern Ocean.

We conducted all analysis in R, version 4.0.3 (R Development Core Team 2020). We implemented the detrending analysis using the ceemdan function in the Rlibeemd library based on the default parameters (Helske and Luukko 2018; Luukko et al. 2016). We implemented beta regression using the betareg function in the betareg library (Cribari-Neto and Zeileis 2010), and Poisson regression using the glm function in the stats library.

3 Results

3.1 Spatial summary

The proportion of each season containing EHE and ECE presented variable patterns across realms and oceans with limited variation between seasons (Figs. 1a–d, 2). Within terrestrial environments, high EHE proportions occurred throughout the Antarctic during both seasons and within the northern latitudes of the Nearctic and Palearctic, especially during the boreal winter (Figs. 1a, 2a–b). High ECE proportions occurred within limited regions of each realm during the boreal summer and across broad regions of the Nearctic and Palearctic during the boreal winter (Figs. 1b, 2c–d). Within marine environments, high EHE proportions occurred within the Arctic Ocean during the boreal winter and within the tropical eastern Pacific and tropical Atlantic during both seasons (Figs. 1c, 2a–b). High ECE proportions occurred across all oceans during both seasons, with the Arctic containing strong seasonal variation and high ECE proportions during the boreal summer (Figs. 1d, 2c–d).

The maximum duration of EHE and ECE presented variable patterns across realms and oceans with limited seasonal variation (Figs. 1e–h, 3). The results for duration largely mirrored those found for proportion as outlined above. Within terrestrial environments, high EHE durations occurred throughout the Antarctic during both seasons and within the northern latitudes of the Nearctic and Palearctic, especially during the boreal winter (Figs. 1e, 3a–b). High ECE durations occurred within limited regions of each realm during the boreal summer and across broad regions of the Nearctic and Palearctic during the boreal winter (Figs. 1f, 3c–d). Within marine environments, high EHE durations occurred within the Arctic Ocean during the boreal winter and within the tropical eastern Pacific and tropical Atlantic during both seasons (Figs. 1g, 3a–b). High ECE durations occurred across all oceans during both seasons, with the Arctic containing strong seasonal variation and high ECE proportions during the boreal summer (Figs. 1h, 3c–d).

3.2 Trend analysis

Trends in the proportion of each season containing EHE and ECE presented variable patterns across realms and oceans with strong seasonal variation (Figs. 4a–d, 5, 6). Within terrestrial environments, significant increases in EHE proportions occurred within the Antarctic and Australasia during both seasons and with the Neotropics and Palearctic during the boreal summer (Figs. 4a, 5, 6). Significant increases in ECE proportions occurred within the

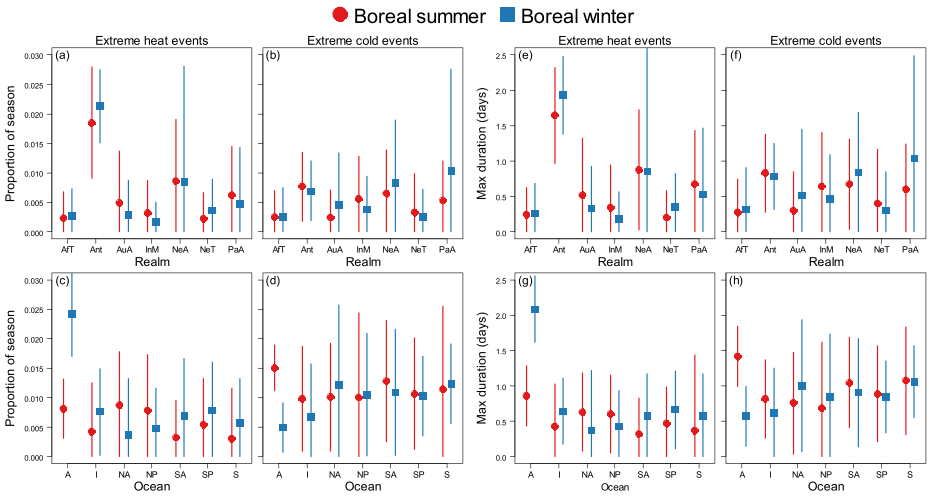

Fig. 1 The median proportion (±2 median absolute deviations) of the boreal summer and boreal winter containing extreme heat events and extreme cold events within **a–b** seven biogeographical realms and **c–d** seven oceans summarized over a 70-year period (1950–2019). The median maximum duration (±2 median absolute deviations) of extreme heat events and extreme cold events during the boreal summer and boreal winter within **e–f** seven biogeographical realms and **g–h** seven oceans summarized over a 70-year period (1950–2019). The seven biogeographical realms include the Afrotropics, Antarctic, Australasia, IndoMalaya, Nearctic, Neotropics, and Palearctic. The seven oceans include the Arctic, Indian, North Atlantic, North Pacific, South Atlantic, South Pacific, and Southern Ocean

Antarctic, Australasia, and Neotropics during both seasons, within the IndoMalaya and Palearctic during the boreal summer, and within the Afrotropics during the boreal winter (Figs. 4b, 5, 6). Within marine environments, significant increases in EHE proportions

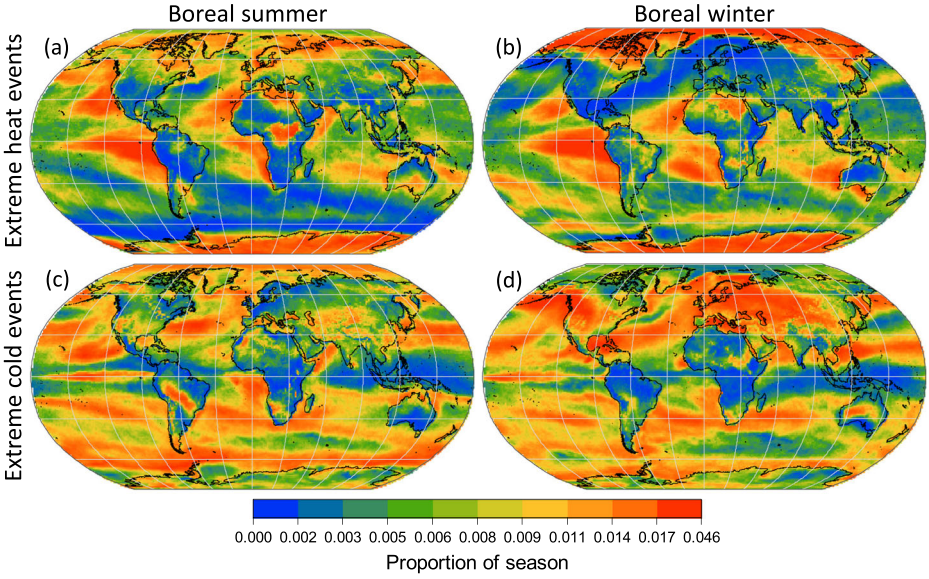

Fig. 2 The average proportion of the **a** boreal summer and **b** boreal winter containing extreme heat events summarized over a 70-year period (1950–2019). The average proportion of the **c** boreal summer and **d** boreal winter containing extreme cold events summarized over a 70-year period (1950–2019)

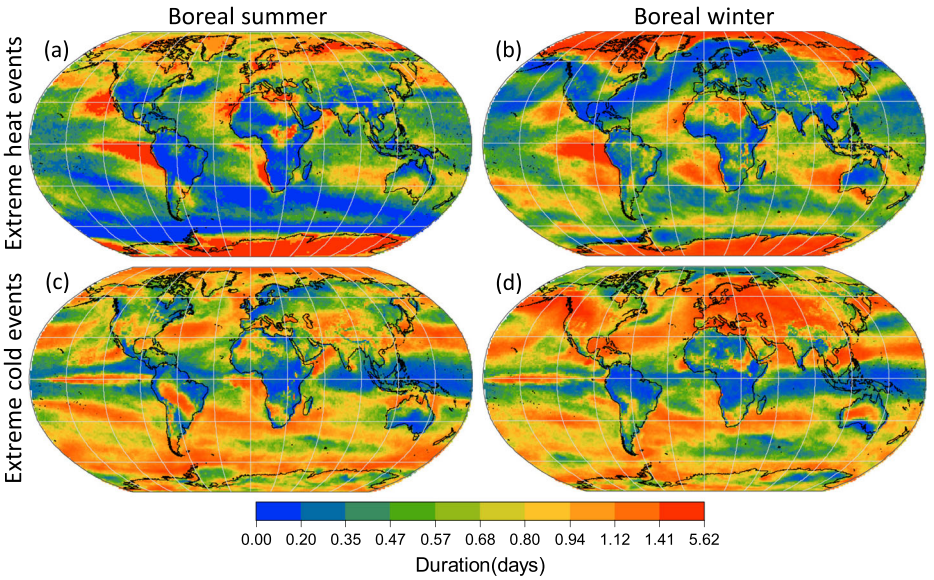

Fig. 3 The average maximum duration (days) during the **a** boreal summer and **b** boreal winter of extreme heat events summarized over a 70-year period (1950–2019). The average maximum duration (days) during the **c** boreal summer and **d** boreal winter of extreme cold events summarized over a 70-year period (1950–2019)

occurred within the Indian Ocean and North Pacific during both seasons, within the North Atlantic and North Pacific during the boreal summer, and South Atlantic and South Pacific during the boreal winter (Figs. 4c, 5, 6). Significant increases in ECE proportions occurred within the Arctic, Indian, South Atlantic, and Southern Ocean during both seasons, within the North Pacific during the boreal summer, and South Pacific during the boreal winter (Figs. 4d, 5, 6).

Trends in the maximum duration of EHE and ECE during each season differed in many cases from those outlined above for proportion of season (Figs. 4e–h, 7, 8). Within terrestrial environments, significant increases in EHE duration occurred within the Antarctic during both seasons and within Australasia during the boreal summer (Figs. 4e, 7, 8). Significant increases in ECE duration occurred within the Antarctic during both seasons and within Australasia, IndoMalaya, and Neotropics during the boreal summer (Figs. 4f, 7, 8). Within marine environments, significant increases in EHE duration occurred within the Indian Ocean and North Pacific during both seasons; within the North Atlantic and North Pacific during the boreal summer; and the Arctic Ocean, South Atlantic, and South Pacific during the boreal winter (Figs. 4g, 7, 8). Significant increases in ECE proportion occurred within the Arctic, Indian, and Southern Oceans during both seasons, within the North Pacific during the boreal summer, and within the South Atlantic and South Pacific during the boreal winter (Figs. 4h, 7, 8).

4 Discussion

Our seasonal assessment of 70 years of detrended temperature data identified global patterns and trends in the frequency and duration of extreme temperature events. Based on our spatial summary, the frequency and duration of EHE and ECE presented similar patterns that

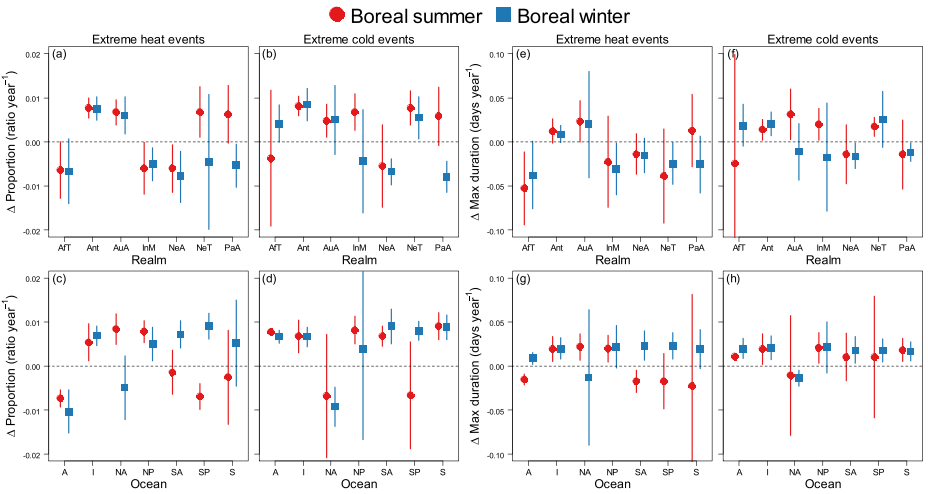

Fig. 4 The median change in the proportion (±2 median absolute deviations) of the boreal summer and boreal winter containing extreme heat events and extreme cold events within **a–b** seven biogeographical realms and **c–d** seven oceans over a 70-year period (1950–2019). The median change in the maximum duration (±2 median absolute deviations) of extreme heat events and extreme cold events during the boreal summer and boreal winter within **e–f** seven biogeographical realms and **g–h** seven oceans over a 70-year period (1950–2019). Only grid cells within each realm and ocean where $P < 0.05$ were included in the calculations (see Figs. 5, 6, 7, 8). The seven biogeographical realms include the Afrotropics, Antarctic, Australasia, IndoMalaya, Nearctic, Neotropics, and Palearctic. The seven oceans include the Arctic, Indian, North Atlantic, North Pacific, South Atlantic, South Pacific, and Southern Ocean

contained limited spatial heterogeneity. High EHE frequency and duration occurred within the Antarctic during both seasons and within the Arctic Ocean during the boreal winter. High ECE frequency and duration occurred within the Nearctic and Palearctic during the boreal winter, and the Arctic Ocean during the boreal summer. Our trend analysis, in contrast, presented

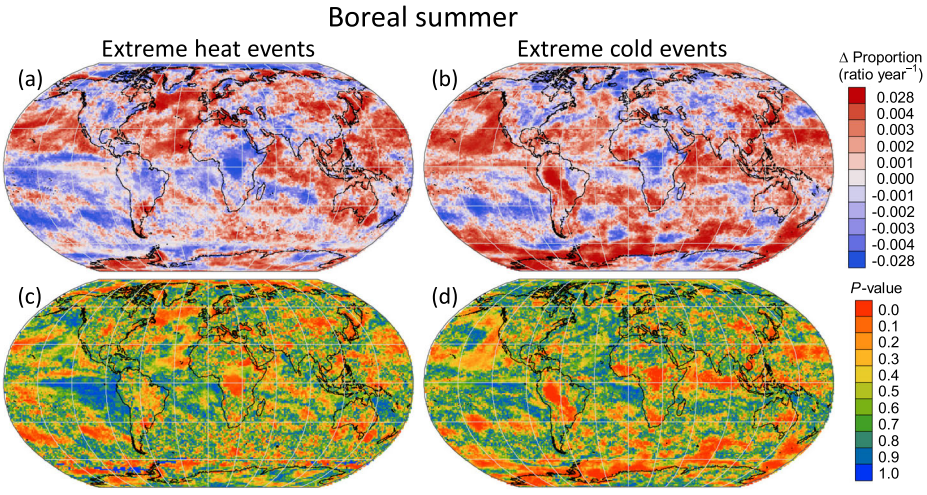

Fig. 5 The change in the proportion of the boreal summer containing **a** extreme heat events and **b** extreme cold events over a 70-year period (1950–2019) estimated using beta regression (units are the ratio of the proportion of extreme events observed to the proportion of extreme events not observed). *P*-values from the beta regression trend estimates for **c** extreme heat events and **d** extreme cold events

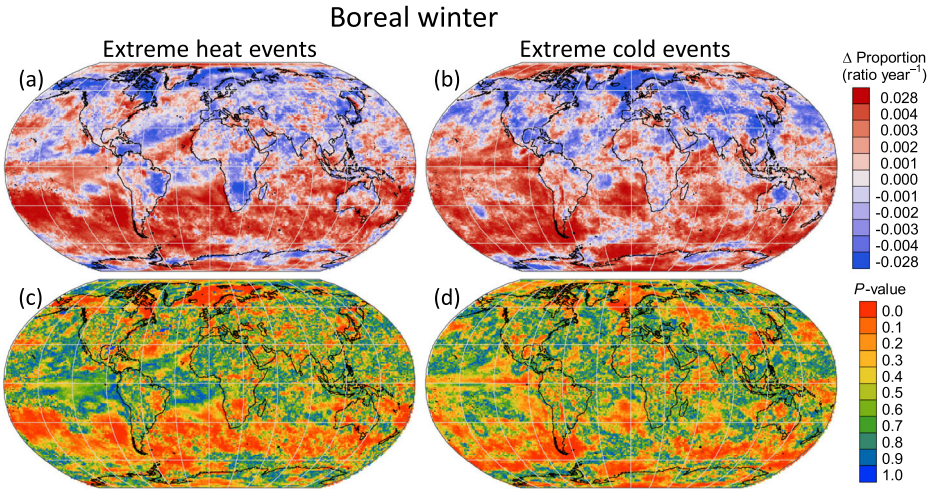

Fig. 6 The change in the proportion of the boreal winter containing **a** extreme heat events and **b** extreme cold events over a 70-year period (1950–2019) estimated using beta regression (units are the ratio of the proportion of extreme events observed to the proportion of extreme events not observed). *P*-values from the beta regression trend estimates for **c** extreme heat events and **d** extreme cold events

pronounced differences between frequency and duration. The trend analysis was characterized by high spatial heterogeneity, especially within terrestrial environments, and strong seasonal differences, particularly between the Northern and Southern Hemispheres. Marine environments tended to contain more consistent positive EHE trends, especially with in the Southern Hemisphere during the austral summer.

A combination of atmospheric mechanisms are often associated with the occurrence of extreme temperature events. This includes mid-latitude blocking events within the Northern Hemisphere that obstruct ambient westerly winds and associated synoptic weather systems.

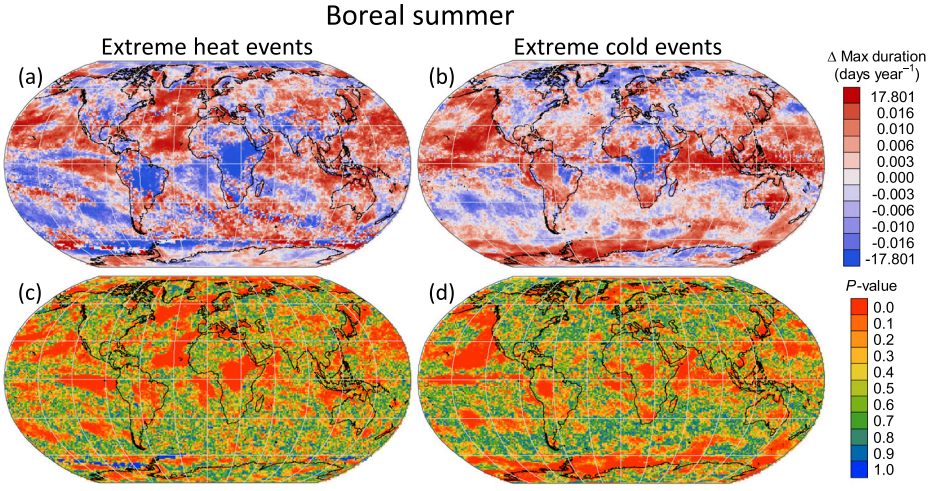

Fig. 7 The change in the maximum duration of **a** extreme heat events and **b** extreme cold events during the boreal summer over a 70-year period (1950–2019) estimated using Poisson regression. *P*-values from the Poisson regression trend estimates for **c** extreme heat events and **d** extreme cold events

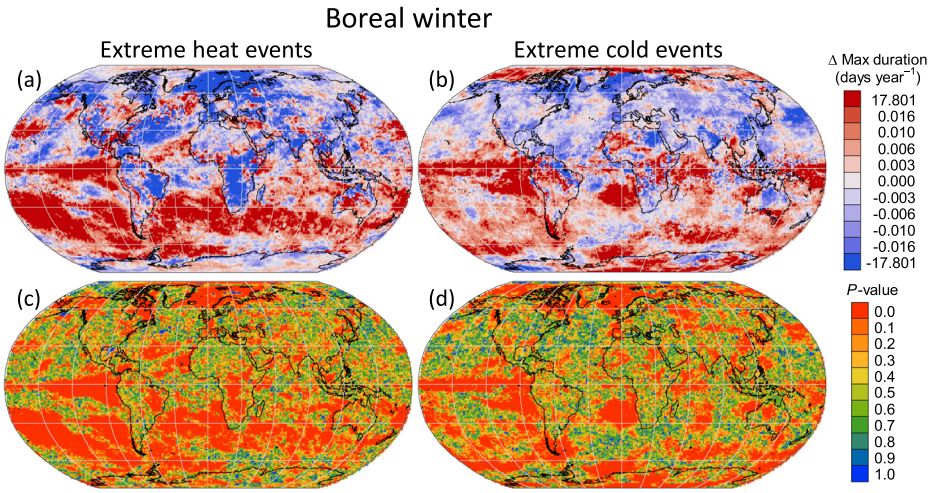

Fig. 8 The change in the maximum duration of **a** extreme heat events and **b** extreme cold events during the boreal winter over a 70-year period (1950–2019) estimated using Poisson regression. *P*-values from the Poisson regression trend estimates for **c** extreme heat events and **d** extreme cold events

Atmospheric blocking can generate extended periods of extreme heat (Pfahl and Wernli 2012; Röthlisberger et al. 2016) or extreme cold (Buehler et al. 2011; Sillmann et al. 2011; Whan et al. 2016). A recurrent Rossby wave pattern may act to enhance the persistence of these blocking events in the Northern Hemisphere (Röthlisberger et al. 2019). Atmospheric blocking also occurs within the mid-latitude of the Southern Hemisphere (Mendes and Cavalcanti 2014), with Northern Hemisphere blocking events tending to be stronger (Lupo et al. 2019). The strongest mid-latitude patterns in our analysis occurred with ECE during the boreal winter within the Northern Hemisphere and with ECE during the austral winter within the Southern Hemisphere. EHE tended to occur at high northern and southern latitudes. Specifically, EHE occurred within Antarctica during the austral summer and winter and within the Arctic Ocean during the boreal winter. Our trend analysis identified positive EHE trends, primarily in duration within marine environments, within the mid-latitudes of the Northern Hemisphere during the boreal summer, and within the mid-latitudes of the Southern Hemisphere during the austral summer. These findings suggest that mid-latitude blocking events may act to enhance the duration of extreme heat events within marine environments in the Northern and Southern Hemispheres.

Our findings identified the tropical eastern Pacific as a region with high EHE frequency and duration during both seasons. This outcome is likely related to the air-sea interactions of the El Niño–Southern Oscillation (ENSO) whose sea surface temperature phases can affect surface air temperatures over the tropical Pacific (Trenberth et al. 2002; Trenberth et al. 2005). The ENSO alternates irregularly between warming (El Niño) and cooling (La Niña) of sea surface temperatures in the tropical eastern Pacific. Current evidence points towards an increasing frequency of extreme El Niño and La Niña events under climate change (Cai et al. 2014; Cai et al. 2015; Wang et al. 2017). Our trend analysis identified increasing EHE and ECE durations within this region, primarily during the boreal winter. In total, these findings highlight the role of ENSO as factor promoting temperature extremes within the tropical eastern Pacific and the potential for these events to increase in duration in the future.

This study provides the first global assessment of ECE patterns and trends within both terrestrial and marine environments. Our findings suggest that ECE frequency and duration are greatest within the mid-latitudes, primarily in the North Hemisphere during the boreal winter. How ECE is being affected by climate change globally has not been fully examined with most studies exploring the patterns and causes of cold-air outbreaks within the mid-latitudes of the Northern Hemisphere (Kolstad et al. 2010; Kretschmer et al. 2018). Our results point to ECE trends that, compared to EHE, are spatially more heterogeneous and contain lower seasonal variation between the Northern and Southern Hemispheres.

In summary, after accounting for the influence of global warming, we documented broad-scale patterns in the frequency and duration of extreme temperature events across the globe. Our trend analysis identified high spatial heterogeneity and strong seasonal variation, with marine environments often presenting more consistent positive trends, especially in the Southern Hemisphere. These results provide the basis to explore the implications of extreme temperature events for human populations (AghaKouchak et al. 2020) and natural systems (Bailey and van de Pol 2016) across terrestrial and marine environments. Our findings emphasize the many near-term challenges that temperature extremes are likely to pose for life on the planet and the need to advance our understanding of the developing long-term implications of these changing dynamics as climate change progresses.

Supplementary Information The online version contains supplementary material available at https://doi.org/10.1007/s10584-021-03094-0.

Acknowledgements We thank two anonymous reviewers for the construction comments on an earlier draft and D. Sheldon and The College of Information and Computer Sciences, University of Massachusetts, for the computational support.

Funding This research was supported by The Wolf Creek Charitable Foundation and the National Science Foundation (DBI-1939187; DEB-2017817).

Declarations

Conflict of interest The authors declare no competing interests.

References

AghaKouchak A et al (2020) Climate extremes and compound hazards in a warming world. Annu Rev Earth Planet Sci 48:519–548. https://doi.org/10.1146/annurev-earth-071719-055228

Alexander LV et al (2006) Global observed changes in daily climate extremes of temperature and precipitation. J Geophys Res Atmos 111:D05109. https://doi.org/10.1029/2005JD006290

Anderson GB, Bell Michelle L (2011) Heat waves in the United States: mortality risk during heat waves and effect modification by heat wave characteristics in 43 U.S. communities. Environ Health Perspect 119:210–218. https://doi.org/10.1289/ehp.1002313

Bailey LD, van de Pol M (2016) Tackling extremes: challenges for ecological and evolutionary research on extreme climatic events. J Anim Ecol 85:85–96. https://doi.org/10.1111/1365-2656.12451

Battisti DS, Naylor RL (2009) Historical warnings of future food insecurity with unprecedented seasonal heat. Science 323:240. https://doi.org/10.1126/science.1164363

Bell B et al (2020) ERA5 hourly data on single levels from 1950 to 1978 (preliminary version). Copernicus climate change service (C3S) climate data store (CDS). (accessed on < 12-01-2020 >), https://cds.climate.

copernicus-climate.eu/cdsapp#!/dataset/reanalysis-era5-single-levels-preliminary-back-extension?tab=overview
Buehler T, Raible CC, Stocker TF (2011) The relationship of winter season North Atlantic blocking frequencies to extreme cold or dry spells in the ERA-40. Tellus A: Dynamic Meteorology and Oceanography 63:174–187. https://doi.org/10.1111/j.1600-0870.2010.00492.x
Cai W et al (2014) Increasing frequency of extreme El Nino events due to greenhouse warming. Nature Clim Change 4:111–116. https://doi.org/10.1038/nclimate2100
Cai W et al (2015) ENSO and greenhouse warming. Nat Clim Chang 5:849–859. https://doi.org/10.1038/nclimate2743
Cayan DR (1980) Large-scale relationships between sea surface temperature and surface air temperature. Mon Weather Rev 108:1293–1301. https://doi.org/10.1175/1520-0493(1980)108<1293:LSRBSS>2.0.CO;2
Colominas MA, Schlotthauer G, Torres M, Flandrin P (2012) Noise-assisted EMD methods in action. Advances in Data Science and Adaptive Analysis:4
Coumou D, Robinson A (2013) Historic and future increase in the global land area affected by monthly heat extremes. Environ Res Lett 8:034018. https://doi.org/10.1088/1748-9326/8/3/034018
Cremonese E, Filippa G, Galvagno M, Siniscalco C, Oddi L, Morra di Cella U, Migliavacca M (2017) Heat wave hinders green wave: the impact of climate extreme on the phenology of a mountain grassland. Agric For Meteorol 247:320–330. https://doi.org/10.1016/j.agrformet.2017.08.016
Cribari-Neto F, Zeileis A (2010) Beta Regression in R. J Stat Softw 34:1–24
Diffenbaugh NS et al (2017) Quantifying the influence of global warming on unprecedented extreme climate events. Proc Natl Acad Sci U S A 114:4881. https://doi.org/10.1073/pnas.1618082114
Fenner D, Holtmann A, Krug A, Scherer D (2019) Heat waves in Berlin and Potsdam, Germany – Long-term trends and comparison of heat wave definitions from 1893 to 2017. Int J Climatol 39:2422–2437. https://doi.org/10.1002/joc.5962
Ferrari S, Cribari-Neto F (2004) Beta regression for modelling rates and proportions. J Appl Stat 31:799–815. https://doi.org/10.1080/0266476042000214501
Fischer EM, Knutti R (2015) Anthropogenic contribution to global occurrence of heavy-precipitation and high-temperature extremes. Nat Clim Chang 5:560. https://doi.org/10.1038/nclimate2617
Flanders Marine Institute (2018) IHO Sea Areas, version 3. Available online at http://www.marineregions.org/. doi:https://doi.org/10.14284/323
Frölicher TL, Fischer EM, Gruber N (2018) Marine heatwaves under global warming. Nature 560:360–364. https://doi.org/10.1038/s41586-018-0383-9
Garrabou J et al (2009) Mass mortality in northwestern Mediterranean rocky benthic communities: effects of the 2003 heat wave. Glob Change Biol 15:1090–1103. https://doi.org/10.1111/j.1365-2486.2008.01823.x
Grant PR, Grant BR, Huey RB, Johnson MTJ, Knoll AH, Schmitt J (2017) Evolution caused by extreme events. Philos Trans R Soc Lond Ser B Biol Sci 372:20160146. https://doi.org/10.1098/rstb.2016.0146
Guo Y et al (2017) Heat wave and mortality: a multicountry, multicommunity study. Environ Health Perspect 125:087006. https://doi.org/10.1289/EHP1026
Gutschick VP, BassiriRad H (2003) Extreme events as shaping physiology, ecology, and evolution of plants: toward a unified definition and evaluation of their consequences. New Phytol 160:21–42. https://doi.org/10.1046/j.1469-8137.2003.00866.x
Harris RMB et al (2018) Biological responses to the press and pulse of climate trends and extreme events. Nat Clim Chang 8:579–587. https://doi.org/10.1038/s41558-018-0187-9
Helske J, Luukko P (2018) Rlibeemd: ensemble empirical mode decomposition (EEMD) and its complete variant (CEEMDAN). R package version 1(4):1 https://github.com/helske/Rlibeemd
Hersbach H et al. (2019a) ERA5 monthly averaged data on single levels from 1979 to present. Copernicus climate change service (C3S) climate data store (CDS). (accessed on < 02-14-2020 >). DOI: https://doi.org/10.24381/cds.f17050d7
Hersbach H et al (2019b) Global reanalysis: goodbye ERA-interim, hello ERA5. ECMWF Newsletter:17–24
Hoffmann L et al (2019) From ERA-interim to ERA5: the considerable impact of ECMWF's next-generation reanalysis on Lagrangian transport simulations. Atmos Chem Phys 19:3097–3124. https://doi.org/10.5194/acp-19-3097-2019
Huang NE et al (1998) The empirical mode decomposition and the Hilbert spectrum for nonlinear and non-stationary time series analysis. P Roy Soc Lond A Mat 454:903–995. https://doi.org/10.1098/rspa.1998.0193
Kolstad EW, Breiteig T, Scaife AA (2010) The association between stratospheric weak polar vortex events and cold air outbreaks in the northern hemisphere. Q J R Meteorol Soc 136:886–893. https://doi.org/10.1002/qj.620
Kretschmer M, Cohen J, Matthias V, Runge J, Coumou D (2018) The different stratospheric influence on cold-extremes in Eurasia and North America. Climate and Atmospheric Science 1:44. https://doi.org/10.1038/s41612-018-0054-4

La Sorte FA, Hochachka WM, Farnsworth A, Dhondt AA, Sheldon D (2016) The implications of mid-latitude climate extremes for north American migratory bird populations. Ecosphere 7:e01261
La Sorte FA, Fink D, Johnston A (2018) Seasonal associations with novel climates for north American migratory bird populations. Ecol Lett 21:845–856. https://doi.org/10.1111/ele.12951
Lambert D (1992) Zero-inflated Poisson regression, with an application to defects in manufacturing. Technometrics 34:1–14. https://doi.org/10.2307/1269547
Lupo AR, Jensen AD, Mokhov II, Timazhev AV, Eichler T, Efe B (2019) Changes in global blocking character in recent decades. Atmosphere 10:92
Luukko PJ, Helske J, Räsänen E (2016) Introducing libeemd: a program package for performing the ensemble empirical mode decomposition. Comput Stat 31:545–557. https://doi.org/10.1007/s00180-015-0603-9
Mair P, Wilcox R (2019) Robust statistical methods in R using the WRS2 package. Beh Res Meth. https://doi.org/10.3758/s13428-019-01246-w
Maron M, McAlpine CA, Watson JEM, Maxwell S, Barnard P (2015) Climate-induced resource bottlenecks exacerbate species vulnerability: a review. Divers Distrib 21:731–743. https://doi.org/10.1111/ddi.12339
Maxwell SL et al (2019) Conservation implications of ecological responses to extreme weather and climate events. Divers Distrib 25:613–625. https://doi.org/10.1111/ddi.12878
McPhillips LE et al (2018) Defining extreme events: a cross-disciplinary review. Earth's Future 6:441–455. https://doi.org/10.1002/2017EF000686
Mendes MCD, Cavalcanti IFA (2014) The relationship between the Antarctic oscillation and blocking events over the South Pacific and Atlantic Oceans. Int J Climatol 34:529–544. https://doi.org/10.1002/joc.3729
Mitchell D et al (2016) Attributing human mortality during extreme heat waves to anthropogenic climate change. Environ Res Lett 11:074006. https://doi.org/10.1088/1748-9326/11/7/074006
Molla MKI, Sumi A, Rahman MS (2007) Analysis of temperature change under global warming impact using empirical mode decomposition. Int J Inf Technol 3:131–139
Oliver ECJ et al (2018) Longer and more frequent marine heatwaves over the past century. Nat Commun 9:1324. https://doi.org/10.1038/s41467-018-03732-9
Olson DM, Dinerstein E (2002) The global 200: priority ecoregions for global conservation. Ann Mo Bot Gard 89:199–224
Oswald EM (2018) An analysis of the prevalence of heat waves in the United States between 1948 and 2015. J Appl Meteorol Clim 57:1535–1549. https://doi.org/10.1175/JAMC-D-17-0274.1
Parker WS (2016) Reanalyses and observations: what's the difference? B Am Meteorol Soc 97:1565–1572. https://doi.org/10.1175/bams-d-14-00226.1
Perkins-Kirkpatrick SE, Lewis SC (2020) Increasing trends in regional heatwaves. Nat Commun 11:3357. https://doi.org/10.1038/s41467-020-16970-7
Pfahl S, Wernli H (2012) Quantifying the relevance of atmospheric blocking for co-located temperature extremes in the Northern Hemisphere on (sub-)daily time scales. Geophys Res Lett 39. https://doi.org/10.1029/2012GL052261
Pielou EC (1979) Biogeography. Wiley, NY
R Development Core Team (2020) R: a language and environment for statistical computing. R Foundation for Statistical Computing https://www.R-project.org/, Vienna, Austria
Röthlisberger M, Pfahl S, Martius O (2016) Regional-scale jet waviness modulates the occurrence of midlatitude weather extremes. Geophys Res Lett 43:10,989–910,997. https://doi.org/10.1002/2016GL070944
Röthlisberger M, Frossard L, Bosart LF, Keyser D, Martius O (2019) Recurrent synoptic-scale Rossby wave patterns and their effect on the persistence of cold and hot spells. J Clim 32:3207–3226. https://doi.org/10.1175/JCLI-D-18-0664.1
Sillmann J, Croci-Maspoli M, Kallache M, Katz RW (2011) Extreme cold winter temperatures in Europe under the influence of North Atlantic atmospheric blocking. J Clim 24:5899–5913. https://doi.org/10.1175/2011JCLI4075.1
Simas AB, Barreto-Souza W, Rocha AV (2010) Improved estimators for a general class of beta regression models. Computational Statistics & Data Analysis 54:348–366. https://doi.org/10.1016/j.csda.2009.08.017
Smale DA et al (2019) Marine heatwaves threaten global biodiversity and the provision of ecosystem services. Nat Clim Chang 9:306–312. https://doi.org/10.1038/s41558-019-0412-1
Smith ET, Sheridan SC (2018) The characteristics of extreme cold events and cold air outbreaks in the eastern United States. Int J Climatol 38:e807–e820. https://doi.org/10.1002/joc.5408
Smith ET, Sheridan SC (2019) The influence of extreme cold events on mortality in the United States. Sci Total Environ 647:342–351. https://doi.org/10.1016/j.scitotenv.2018.07.466
Smith TT, Zaitchik BF, Gohlke JM (2013) Heat waves in the United States: definitions, patterns and trends. Clim Chang 118:811–825. https://doi.org/10.1007/s10584-012-0659-2
Smithson M, Verkuilen J (2006) A better lemon squeezer? Maximum-likelihood regression with beta-distributed dependent variables. Psychol Methods 11:54–71. https://doi.org/10.1037/1082-989X.11.1.54

Stallone A, Cicone A, Materassi M (2020) New insights and best practices for the successful use of empirical mode decomposition, iterative filtering and derived algorithms. Sci Rep 10:15161. https://doi.org/10.1038/s41598-020-72193-2

Torres ME, Colominas MA, Schlotthauer G, Flandrin P (2011) A complete ensemble empirical mode decomposition with adaptive noise. In: 2011 IEEE International Conference on Acoustics, Speech and Signal Processing (ICASSP), pp 4144–4147. https://doi.org/10.1109/ICASSP.2011.5947265

Trenberth KE, Caron JM, Stepaniak DP, Worley S (2002) Evolution of El Niño–Southern oscillation and global atmospheric surface temperatures. J Geophys Res Atmos 107:AAC 5–1-AAC 5–17. https://doi.org/10.1029/2000JD000298

Trenberth KE, Stepaniak DP, Smith L (2005) Interannual variability of patterns of atmospheric mass distribution. J Clim 18:2812–2825. https://doi.org/10.1175/jcli3333.1

Walsh JE, Phillips AS, Portis DH, Chapman WL (2001) Extreme cold outbreaks in the United States and Europe, 1948–99. J Clim 14:2642–2658. https://doi.org/10.1175/1520-0442(2001)014<2642:ECOITU>2.0.CO;2

Wang G et al (2017) Continued increase of extreme El Niño frequency long after 1.5 °C warming stabilization. Nat Clim Chang 7:568–572. https://doi.org/10.1038/nclimate3351

Warton DI, Lyons M, Stoklosa J, Ives AR (2016) Three points to consider when choosing a LM or GLM test for count data. Methods Ecol Evol 7:882–890. https://doi.org/10.1111/2041-210X.12552

Weiss NA (2015) wPerm: permutation tests. R package version 1.0.1. https://CRAN.R-project.org/package=wPerm

Wernberg T et al (2013) An extreme climatic event alters marine ecosystem structure in a global biodiversity hotspot. Nat Clim Chang 3:78–82. https://doi.org/10.1038/nclimate1627

Whan K, Zwiers F, Sillmann J (2016) The influence of atmospheric blocking on extreme winter minimum temperatures in North America. J Clim 29:4361–4381. https://doi.org/10.1175/JCLI-D-15-0493.1

Wheeler DD, Harvey VL, Atkinson DE, Collins RL, Mills MJ (2011) A climatology of cold air outbreaks over North America: WACCM and ERA-40 comparison and analysis. J Geophys Res Atmos 116. https://doi.org/10.1029/2011JD015711

Williams JW, Jackson ST (2007) Novel climates, no-analog communities, and ecological surprises. Front Ecol Environ 5:475–482

Williams JW, Jackson ST, Kutzbach JE (2007) Projected distributions of novel and disappearing climates by 2100 AD. Proc Natl Acad Sci U S A 104:5738–5742

Wood SN (2017) Generalized additive models: an introduction with R, 2nd edn. Chapman & Hall/CRC, Boca Raton, FL

Wu Z, Huang NE (2009) Ensemble empirical mode decomposition: a noise-assisted data analysis method. Adv Adapt Data Anal 01:1–41. https://doi.org/10.1142/s1793536909000047

Wu Z, Huang NE, Long SR, Peng C-K (2007) On the trend, detrending, and variability of nonlinear and nonstationary time series. Proc Natl Acad Sci U S A 104:14889. https://doi.org/10.1073/pnas.0701020104